Journal of Pharmaceutical and Biomedical Analysis 149 (2018) 603–611

Contents lists available at ScienceDirect

Journal of Pharmaceutical and Biomedical Analysis

journal homepage: www.elsevier.com/locate/jpba

Assessment of mefenamic acid polymorphs in commercial tablets using chemometric coupled to MIR and NIR spectroscopies. Prediction of dissolution performance

Marina Antonio [a], Rubén M. Maggio [a,b,*]

[a] Área de Análisis de Medicamentos, Facultad de Ciencias Bioquímicas y Farmacéuticas, Universidad Nacional de Rosario, Suipacha 531, Rosario S2002LRK, Argentina
[b] Instituto de Química Rosario (IQUIR, CONICET-UNR), Suipacha 531, Rosario S2002LRK, Argentina

ARTICLE INFO

Article history:
Received 8 September 2017
Received in revised form
22 November 2017
Accepted 24 November 2017
Available online 28 November 2017

ABSTRACT

Mefenamic Acid (MFA) is a widely-used non-steroidal anti-inflammatory drug. MFA presents four possible crystal forms; Form I and Form II being the only two pure crystals that have been isolated and fully characterized. Both Form I and Form II were prepared following the literature and completely characterized by middle (MIR) and near (NIR) infrared spectroscopy, digital optical microscopy, differential scanning calorimetry, melting point and dissolution properties. In order to develop quantitative models to assess Form I in formulated products, two sets of samples, training (n = 10) and validation (n = 8) sets, were prepared by mixing both polymorphs and the matrix of excipient (simulating commercial tablets). The particle size of the samples was homogenized by sieving and samples were mechanically mixed. A batch of commercial tablets was gently disaggregated, sieved and mechanically mixed for further analysis. For each sample, full MIR and NIR spectra were acquired and used as input of partial least squares (PLS) algorithm separately. Method optimization and internal validation were performed by leave one out procedure. Full spectra and 5 PLS-factors were used for MIR; while, 5 PLS-factors and mean center spectra of full spectra were the optimal conditions for NIR. Accuracy and precision were assessed by evaluation of the actual vs. predicted curve of validation set; and by calculating validation set recoveries and deviations (104.3 ± 8.2% and 100.4 ± 1.0% for MIR and NIR respectively). Only NIR-PLS yielded acceptable results and low deviations during commercial samples evaluation (102.8 ± 0.1%). The same behavior was observed when spiked tablets were analyzed (103.5 ± 0.5%). Additionally, for the calibration set ten dissolution profiles (average of 6 curves each), were obtained under optimized test conditions (900 ml of buffer phosphate pH 9 with surfactant, apparatus II USP, 100 rpm, detection at 342 nm). A multiple linear regression (MLR) was carried out using dissolution profiles and Form I content. The developed MLR model could correlate dissolution profiles and polymorphic richness. This approach, coupled to previously developed NIR-PLS, may act as a valid tool to estimate dissolution profiles from solid forms.

1. Introduction

Crystal polymorphism is the ability of a solid material to exist in more than one crystal form or structure, all of them with the same chemical composition. Polymorphism affects the world of the pharmaceutical industry, where it generates a significant number of patents. The importance of polymorphism is due to the different properties of solid forms, as solubility, powder compaction capacity, flow properties and stability. These differences may finally affect the bioavailability of the drug and show therapeutic implications [1].

Mefenamic Acid (MFA) is 2-(2,3-dimethylphenyl) aminobenzoic acid (Fig. 1A). This non-steroidal anti-inflammatory drug is used worldwide to treat mild to moderate pain, including headache, dental pain, dysmenorrhea, rheumatoid arthritis, osteoarthritis and other disorders [2–4]. MFA presents problems in granulation, tableting, and dissolution due to its poor solubility, high hydrophobicity, and tendency to stick to surfaces [5–7].

Additionally, MFA exists as dimorphs, Form I and Form II. Besides, metastable co-crystals with adenine and cytosine have also

* Corresponding author at: Área de Análisis de Medicamentos, Facultad de Ciencias Bioquímicas y Farmacéuticas, Universidad Nacional de Rosario, Suipacha 531, Rosario S2002LRK, Argentina.
E-mail address: maggio@iquir-conicet.gov.ar (R.M. Maggio).

https://doi.org/10.1016/j.jpba.2017.11.053
0731-7085/

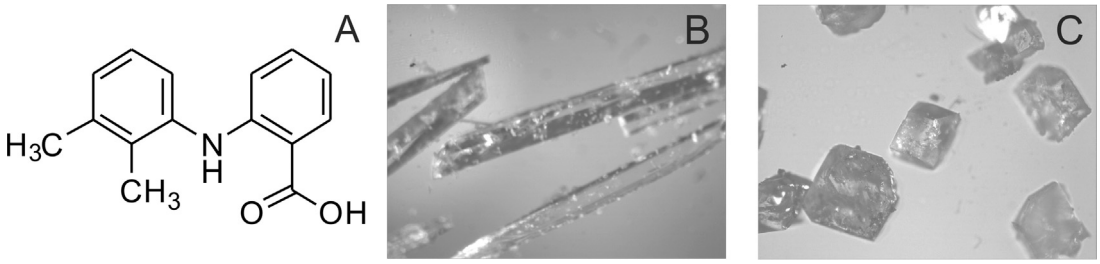

Fig. 1. Chemical structure of the acid form of MFA (A). Images of the crystals obtained by digital optical microscopy for Form I (B) and Form II (C), using a total magnification of 200×.

been reported, as well as a dimethylformamide (DMF) solvate [8]. Nevertheless, Form I and Form II are the only pure forms that have been isolated and fully characterized [9,10].

In most cases, drug specifications in pharmacopoeias include information about identification, purity and assay, but only the European Pharmacopoeia includes a warning about MFA polymorphism [11]. Usually, the most stable crystalline form is the first choice when formulating an active pharmaceutical ingredient (API). However, a more soluble form (usually a less-stable one), is chosen when an API belongs to Class II or III of the Biopharmaceutical Classification System, as in the case of MFA [12,13].

Thus, the change of polymorph in the formulated products may occur by an inadvertent crystallization of amorphous API or a conversion between two crystalline forms. A research group reported solid-form conversion of MFA from Form II to Form I in microemulsions of DMF [14]. High humidity conditions also promote Form II to Form I transformation in solvents suspensions and pure solids of MFA [15]. In addition, the presence of Form I crystals shortened both nuclei formation and growth processes. A solid phase conversion of Form II to Form I after equilibration with the solvents was also reported [16].

These transformation phenomena may alter the quality of the medication; especially when polymorphs have different dissolution properties. MFA pure forms differ in solubility and stability. These variations solubility are due to the different crystalline structures, where Form II has larger dissolution rates and saturation concentrations than Form I in several solvent systems [17,18]. Several attempts to improve MFA solubility were carried out using solid dispersions with polyoxyethylene–polyoxypropylene [19], polyethyleneglycol 400 [20], polyvinylpyrrolidone and crospovidone [21]. A freeze-drying procedure was also used to improve the solubility performance of MFA [22].

Therefore, it is crucial to characterize the crystalline form of MFA, in order to find the implications in the dissolution performance and to develop methodologies for polymorph determination [23]. Several analytical approaches were carried out to determine MFA polymorphs. In order to fully characterize the MFA polymorphic forms, Cesur and Gokbel used the scanning electron microscopy, Raman and X-ray diffraction to characterize and assign polymorph in the API [24].

A quantitative approach based on MIR spectroscopy method has been developed [25]. The model was used to study the thermal conversion of MFA from its Form I to the Form II. However, it has the drawback that it is based on univariate determination, prone to interferences from excipients. Polymorphism identification and determination have been addresses by several approaches; among these, chemometrics have proved to be a valid tool to such complex task [26]. Partial least square (PLS) regression coupled to THz-spectrometry was used to measure polymorphic content in a bulk powder, of MFA [27]. However, no chemometric approaches were found to quantitate polymorphic content in pharmaceutical formulations.

The aim of this work was to use the differential features in MIR and NIR spectra of Form I and Form II in order to develop quantitative analytical methodology for polymorphic content by a chemometric method. Dissolution performance of the polymorphs and their mixtures was also explored and analyzed by multivariate methodology in order to provide a model able to estimate dissolution behavior. The scope and limitations of the methods were also analyzed using real samples.

2. Material and methods

2.1. Instrumentation

Digital optical microscopy of the crystal forms was carried out with the aid of an optical microscope (Seiwa Optical, Tokyo, Japan), fitted with 10 ×, 40 × and 100 × objectives and as ocular a 5 × Beion CMOS digital camera of 5.0 megapixels [Shanghai Beion Medical Technology Co., Ltd., Shangai, China; resolution 2592 × 1944 (H × V)].

A Shimadzu model DSC60 differential scanning calorimeter (Shimadzu Corp., Kyoto, Japan), was used to perform calorimetric determinations. The samples (∼5 mg) were placed in closed aluminum pans perforated with a pinhole to equilibrate pressures. Closed pans were heated at 5 °C min^{-1} between 30 and 300 °C, under a constant flow of nitrogen (50 ml min^{-1}). An empty aluminum pan was used as a reference.

The melting points were determined with an IONOMEX melting point instrument (IONOMEX, Buenos Aires, Argentina). The samples were heated at 10 °C min^{-1} up to 195 °C; then, the heating rate was changed to 1 °C min^{-1}.

The MIR spectra were acquired in a Shimadzu Prestige 21 FT-IR spectrometer (Shimadzu Corp., Kyoto, Japan) over a wavenumber range of 3800–600 cm^{-1} with a resolution of 4 cm^{-1}, using a diamond-based ATR accessory (GladiATR, Pike Technologies, Madison, USA) fitted with a Pike temperature control unit. To achieve a sufficient signal to noise ratio, samples were measured in triplicate.

The NIR spectra were measured at room temperature in reflectance mode with a spectrometer NIRS DS2500 FOSS (FOSS, Hillerod, Dinamarca). Every sample (700 mg) was placed in a circular quartz cell for solids, samples were measured in triplicate and NIR spectra were collected in the spectral range 400–2500 nm.

The dissolution tests were carried out using a Hanson SR8-Plus dissolution station (Hanson Research, Chatsworth, USA), configured as USP apparatus II (paddles) [28] and a paddle rotation rate of 100 rpm. The dissolutions were performed in 900 ml of selected dissolution medium thermostatized at 37 °C. The dissolution medium was previously degassed by sonication. Aliquots of 3 ml were taken without replacement, at pre-established times. The amount of dissolved MFA was determined by spectroscopic measures at 342 nm using an Agilent 8453 UV–DAD spectrophotometer (Agilent Technologies, Santa Clara, USA). Determinations were performed in a quartz cell (10 mm optical path length) against a blank of dis-

solution media. Each dissolution test comprised 6 repetitions of dissolution.

The particle size of the solid samples was standardized by sieving, employing a Zonytest EJR 2000 fine mesh vertical vibratory sieving tower (Rey & Ronzoni, Buenos Aires, Argentina), operating at 1200 rpm. In all cases, the 100–140 mesh fractions were collected.

The physical mixtures of solids were homogenized using a Z-mixer moved by rotatory platform with an electronic control of speed Precytec AT-15D, at 30 rpm for 30 min.

2.2. Chemicals

The MFA pharmaceutical grade (COM) was a kind gift from Laboratorios ELEA (Buenos Aires, Argentina). The excipients (methylcellulose, cornstarch, silicon dioxide, microcrystalline cellulose, sodium croscarmellose, and magnesium stearate) were of pharmaceutical grade and were purchased from "Droguería Saporiti" (Buenos Aires, Argentina). Commercial tablets containing 500 mg of MFA (average total weight: 713.91 mg) were purchased from a local pharmacy.

All other chemicals were of analytical grade and were used as received. During the experiments, the API and its forms were kept in a desiccator and protected from light.

2.2.1. Dissolution media

Monobasic phosphate solutions of potassium and NaOH were prepared both with a concentration of 0.2 M. Phosphate solution (500 ml) was transferred to a 2000 ml beaker, 470 ml of the NaOH solution to obtain a pH of 8 or 9. When surfactant was required subsequently, 35 g of sodium lauryl sulfate was added, maintaining constant agitation until complete dissolution.

2.3. Preparation of the MFA crystal forms

To obtain Form I, approximately 5 g of MFA were weighed and dissolved in 190 ml of 5N NaOH. Then, HCl 6.6 N was added dropwise until pH 2 was reached, under constant mechanical stirring. The formation of a white precipitate was immediately observed. It was allowed to decant overnight (4 °C) to promote the formation of crystals. Finally, it was filtered under vacuum and the residue was placed in a vacuum oven (60 °C) to completely remove the moisture content.

Form II was obtained by a slight modification of the literature [10]. Six MFA aliquots (200 mg) were placed in hermetical glass tubes, under N_2 atmosphere, and heated to 160 °C for 48 h. Then temperature was raised up to 180 °C and held constant for 24 h. Once obtained, the polymorphs were kept in a desiccator at room temperature, protected from light.

2.4. Samples preparation

In order to develop a quantitative method for the determination of purity of Form I in commercial products, we proceeded to prepare training (calibration) and validation samples containing different mixtures of both polymorphs, and excipients in proportions equivalent to commercial tablets.

2.4.1. Matrix of excipients

The excipient matrix was used to simulate the commercial tablets environment. It was prepared by weighing and mixing the following components: methylcellulose (9.55 g), cornstarch (95.53 g), silicon dioxide (2.00 g), microcrystalline cellulose (96.61 g), croscarmellose sodium (3.52 g), sodium lauryl sulfate (8.90 g) and magnesium stearate (2.00 g). The sample size of each excipient was previously homogenized by sieving, collecting the fractions comprised between 100 and 140 mesh. Subsequently, the mechanical mixing of the components was carried out.

2.4.2. Model samples for quantitative analysis

The training and validation sets of samples contained five levels: 0.750, 0.800, 0.850, 0.900, and 1.00 w/w; and four levels: 0.780, 0.830, 0.880 and 0.9500 w/w, Form I/total MFA. The weigh was completed with excipient matrix to obtain MFA/Excipients ratio of 500 mg/212.18 mg, respectively and to reach the weight of 1.424 g for each sample. Subsequently, the mechanical mixing of the components was carried out for 30 min. Both sets were prepared in duplicate, rendering a grand total of 18 samples. As commercial MFA proved to be Form I along its characterization (*4.1. Characterization of the solid forms*), commercial MFA was used for model sample preparation.

2.4.3. Commercial samples

Ten tablets were randomly chosen. For each tablet, the cover was removed and the tablet core was gently disintegrated and reduced to powder, in order to avoid polymorphic conversions. Particle size was homogenized by sieving, collecting 100–140 mesh fractions.

2.4.4. Spiked commercial samples

An aliquot of the samples obtained in Section 2.4.3 was used for the preparation of samples of spiked commercial tablets. A proportion corresponding to 15% of the Form II was added to powdered samples. The appropriate content of excipients was also added. The mixtures were treated similarly to the training and validation sets.

2.5. Chemometrics and graphics software

Exploratory analysis of data, statistics and graphs were performed using Origin 8.0 (OriginLab Co., Northampton, USA) and Microsoft office Excel 2003 (Microsoft, Redmond, USA).

PLS calculation were carried out using MVC1 Toolbox available from (http://www.iquir-conicet.gov.ar/descargas/mvc1.rar) run in Matlab R2010a (Mathworks, Natick, USA). Multiple linear regression (MLR) calculations were carried out using Design-Expert 7.0 (Stat-Ease, Minneapolis, USA).

3. Results and discussion

3.1. Characterization of the solid forms

The polymorphs of MFA were obtained according to Section 2.3. Preparation and designation of the MFA crystal forms was carried out according to Aguiar and Zelmer [17]. The characterization was performed by optical microscopy, MIR and NIR spectroscopy, melting point determination, differential scanning calorimetry, and dissolution properties.

Observations with the optical microscope revealed the crystalline habits of MFA polymorphs (Fig. 1B and C). Form I appears as crystals in the form of well-defined yellowish-colored needles. On the other hand, Form II exhibits prismatic grayish crystals, in agreement with the literature [10]. COM showed a very small particle size, making the microscopic determination impossible.

When the melting point was determined, it was similar for COM (195–200 °C) and Form I (200–205 °C), but Form II melted at higher temperatures (215–220 °C). Likewise, when DSC analysis was performed (Fig. 2), two endothermic peaks were observed for Form I at 170 °C and 238 °C, both related to the transformation of Form I to Form II and fusion (as Form II) respectively. In the case of COM, a similar behavior was observed: a transformation followed by a fusion. The Form II exhibited a single endothermic peak at 233 °C, which is associated with its melting point. The values obtained were in agreement with data described in the literature [29,30].

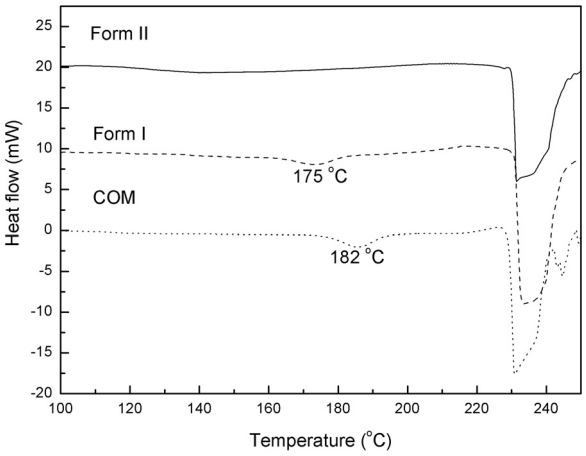

Fig. 2. DSC thermograms of MFA, COM (·), Form I (- -) and Form II (-).

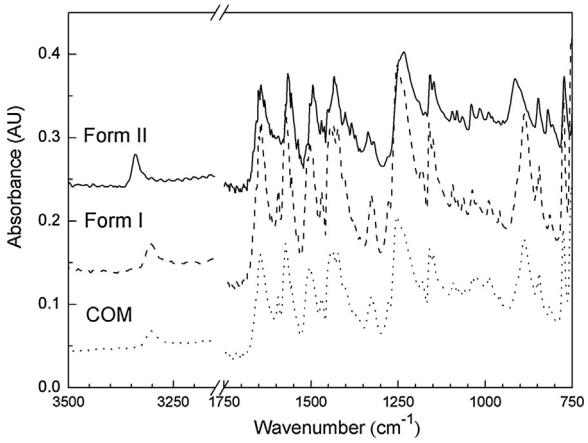

Fig. 3. MIR spectra of MFA, COM (·), Form I (- -) and Form II (-).

MIR spectra of MFA polymorphs were divided in three main regions for further analysis: 3500–1800 cm^{-1}, 1800–1650 cm^{-1} and fingerprinting region (1650–750 cm^{-1}). First, region 3500–1800 cm^{-1} contains many signals but only a relevant peak for MFA polymorphism located around 3350 cm^{-1} in Form II or 3311 cm^{-1} in Form I, in agreement with the literature [31].

In the second region 1800–1650 cm^{-1}, there are no substantial differences; whereas in the fingerprinting region, there are many small differences, which are still important for polymorph classification. A detailed analysis of differences on the MIR spectra and bands assignation is shown in Table 1. Additionally, we checked for pressure-mediated polymorph-transformations, in both Form I and Form II, by repetitive measures in ATR plate. No transformations were found, validating the technic for further analysis.

When MIR spectrum of COM was analyzed (Fig. 3), it proved to be quite similar to Form I regarding the position and the intensity of the peaks. This observation, together with the thermal analysis, allows us to infer that the crystalline structure present in COM is Form I. Peaks at 2926 cm^{-1} and 2900 cm^{-1} had different intensities in each polymorph. The same phenomenon can be observed in peaks at 1619 cm^{-1} and 1600 cm^{-1} or 1574.8 cm^{-1} and 1537.7 cm^{-1}. A peak at 1360 cm^{-1} was typically found in Form I while a shoulder at 1324 cm^{-1} was characteristic for Form II. A small peak found at 1120 cm^{-1} in Form I, shifted to 1130 cm^{-1} in Form II.

Furthermore, differences were observed among the three peaks between 898 cm^{-1} and 786 cm^{-1}.which that have different intensities in each polymorph. On the other hand, the peaks at 768 cm^{-1} and 756 cm^{-1} were found to be typical of Form II and only a peak in Form I was found in this region (764 cm^{-1}). Peaks at 718 cm^{-1} and 637 cm^{-1} are only present in Form I and the signal at 696 cm^{-1} is lower in intensity in Form I than in Form II. Since minor but critical differences in the MIR spectra are present in both polymorphs (Table 1), it would be feasible to set up an analytical methodology based on MIR spectra to quantitate the polymorphs. This fact encouraged the development of a method for quantitative analysis of Form I by coupling chemometrics and MIR.

Fig. 4 shows the graphs of NIR spectra obtained for COM, Form I and Form II. It can be seen that regions with the greatest spectral differences are located between 2000 and 2500 nm. However, both polymorphs showed differences through the entire spectral range. Table 2 summarizes Form I and Form II the major signals, and their tentative assignation. Among these signals, peaks at 1566 and 2366 nm in Form I and those at 1533 and 2109 nm in Form II are to be highlighted. Additionally, changes in peak formations (unresolved, double and triple peaks) between both polymorphs were observed in the entire spectra. NIR spectrum of COM was fully coincident with Form I, reinforcing the idea that the polymorph present in commercial API is Form I.

Table 1
Main signals and differences in the MIR spectra of Forms I and II of MFA.

Form I		Form II		Assignation
Signal (cm^{-1})		Signal (cm^{-1})		
peak	3311	peak	3340	NH vibration
peak (++)	1643	peak (+)	1643	C=O stretching
small peak	1593	–	–	benzene ring stretching
peak	1570	peak	1564	
peak	1508	shoulder + peak	1492	
peak	1469	double peak	1496–1492	C—H or ring
triple peak	1442–1441	peak	1433	deformation
shoulder	1402	peak	1402	
–	–	peak	1382	Anti-symmetric CH_3
peak	1327	double peak	1336–1319	and CH_3' stretching
small peak	1276	–	–	
peak	1251	peak	1230	
small peak	958	–	–	Out-of-plane CH
peak	912	peak	885	deformation
shoulder + peak	844	peak	848	
peak	815	peak + shoulder	819	
sharp peak	775	wide peak	773	Ring deformation and
double peak	752–744	peak	742	CO_2 wagging

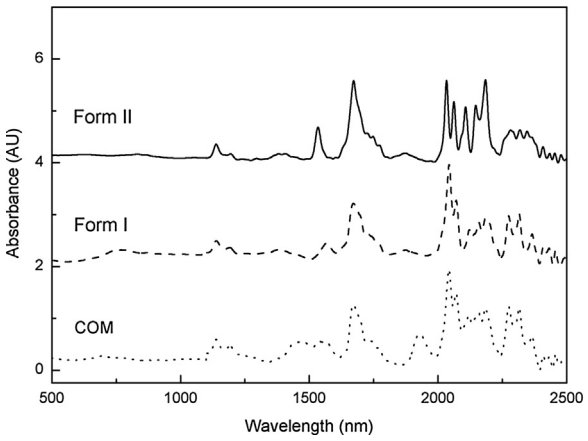

Fig. 4. NIR spectra of MFA, COM (·), Form I (- -) and Form II (-).

3.1.1. Dissolution behavior of polymorph and discriminant dissolution media

The dissolution behavior of polymorphs was assessed as a functional characterization step. Taking into account poor solubility of MFA and the recommendations some international pharmacopoeias [28], basic media and surfactants were used to carry out this test. Four different dissolution media were tested; buffer phosphate media at pH 8 and 9, both with and without the use of sodium lauryl sulfate (SLS) as surfactant. Other experimental conditions are described in Material and Method section (2.1 and 2.2.1).

Fig. 5 shows the behavior of COM, Form I and Form II (Fig. 5A–C) at the different dissolution media. Form I shows almost a similar behavior in the four media, but pH 8 without SLS showed poorer dissolution rates. The final dissolution (at 120 min) ranged from 55 to 75% of the dissolved mass. When Form II was analyzed, a large dispersion of the dissolution rates was observed. A significant dissolution was only observed at pH 9 with SLS, yielding only a 45% of mass dissolved. When dissolution of COM was analyzed, the presence of SLS showed a great influence on the MFA solubility at both pHs (dissolution rates about 80%).

Analyzing the three solids at pH 9 with SLS (the most favored media for all species) dissolution profiles were in the range from 40% to 80% of the mass dissolved, but still showing substantial differences that would allow their discrimination (Fig. 5D).

3.2. Method development to assess polymorph content, quantitative approach

In order to develop models to quantitate MFA forms present in the formulated products, several sets of samples were prepared according to the procedure described in Section 2.4.

Model samples (Calibration, Validation, and Commercial samples) were scanned by MIR and NIR spectroscopies. PLS algorithm was used to evaluate the data obtained from the different analytical techniques (NIR and MIR separetely). Dissolution profiles were obtained from calibration samples and MLR was applied to analyze dissolution profiles in order to see if they are related to the polymorphic content.

3.2.1. NIR data analysis

During the characterization of solid forms (Section 4.1), NIR spectra showed critical differences that allow polymorph resolution in the pure forms (Table 2). However, the presence of excipients may interfere with such task in the formulated products, where the multivariate tool appears as a valid solution. Thus, PLS was proposed to analyze NIR spectra for the quantitate Form I in the presence of Form II and excipients.

NIR spectra were obtained in the 400–2500 nm spectral range, each sample was measured by in triplicate and the spectra obtained were averaged. This procedure was repeated twice, yielding a total of 20 spectra for the calibration set and 16 for the validation set.

The PLS method was developed following three main steps: calibration/optimization, internal/external validation and commercial sample evaluation.

The calibration and optimization of PLS where carried out with the spectra of calibration set by a cross-validation procedure (leave-one-out). The optimal parameters were found following the criterion of minimum PRESS (Prediction Error Sum of Squares). Mean centering pretreatment, five PLS factors and 400–2500 nm spectral range were selected as optimal parameters. Table 3 summarizes the PLS critical parameters and figures of merits obtained during cross-validation.

Internal validation was carried out by analyzing figures of merits (Table 3), in order to verify whether the method is suitable for the scope proposed. An r^2 value higher than 0.950 and a low RMSD value assure a good fitting of the model to NIR data. Additionally, a high analytical sensibility and a LOQ (0.10% W/W) seven times lower than the minimum concentration of the calibration range reinforce the idea of method suitablitity.

The Accuracy and precision of the method were assessed during the evaluation of the validation set of samples (external validation). Eight samples were analyzed in duplicate and

Table 2
Main signals and differences in the NIR spectra of MFA Form I and II.

Form I		Form II		
Signal	(nm)	Signal	(nm)	
peak	417	peak	428	Visible
peak	1566	peak	1533	1st overtone NH
unresolved peaks	2044	unresolved peaks	2034	1st overtone C=O
	2072		2062	
unresolved peaks	2124	peak	2109	
	2161	unresolved peaks	2149	NH combinations
	2190		2186	
peak	2276	unresolved peaks	2282	CH/CH_3 combinations
Shoulder + peak	2317		2319	
–			2348	
peak	2366	–	–	
double peak	2410	peak	2410	
	2432	peak	2435	
peak	2458	peak	2455	
		peak	2479	

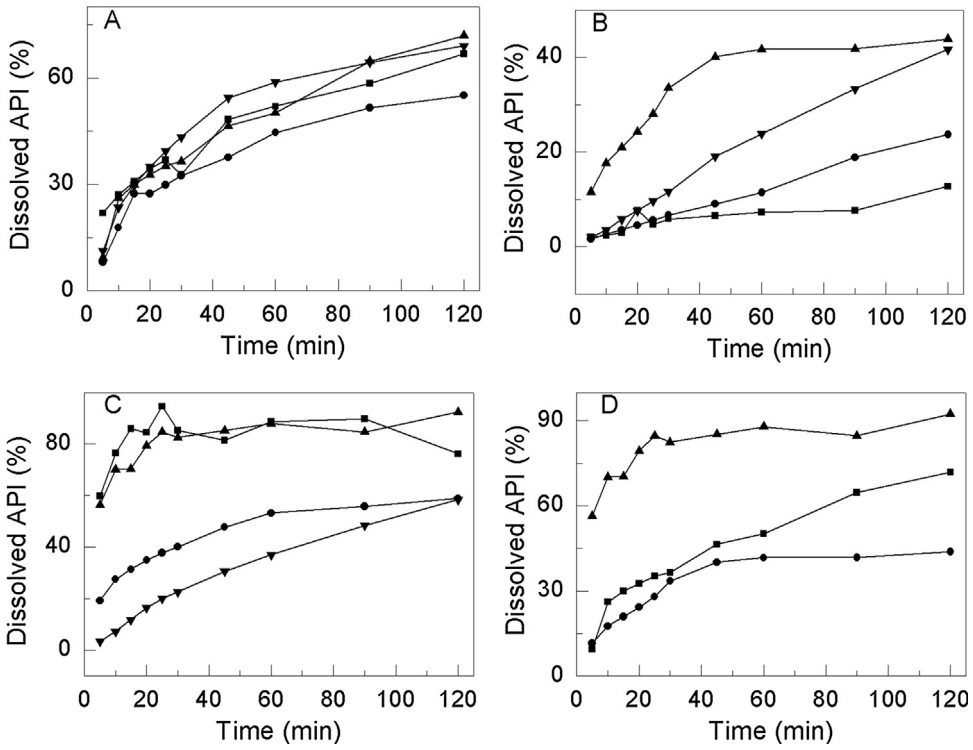

Fig. 5. Dissolution profile of Form I (A), Form II (B) and COM(C) in phosphate medium at pH 8 with (■) or without SLS (●) and at pH 9 with (▲) or without SLS (▼). Comparison of Form I (●), Form II (■) and COM (▲) at pH 9 with SLS (D).

an actual vs. predicted curve was constructed (Fig. 6A). The overall recovery was not statistically different from to 100% [$T_{calculated} = 1.54, T_{(0.99;Df=15)} = 2.61$] and SD was lower than 2% ($100.4 \pm 1.0\%$), showing accurate results and low dispersions. Additionally, when the curve was visualized predicted the values were placed close to the ideal curve (slope 1 and intercept 0), showing the absence of systematic and bias errors (Fig. 6C).

Once PLS was fully validated, the polymorphic content of the commercial tablets was analyzed (Section 2.4.3). Three spectra per samples were acquired and averaged; samples were analyzed in quadruplicate.

The estimated value of Form I for the tablets was 1.028 ± 0.001 w/w and agreed the API used by the manufacturer. The validated model was also used to estimate the polymorphic content of spiked commercial samples (0.880 ± 0.005 w/w), where recoveries were almost quantitative 103.5% with respect to the actual value (0.850, w/w), as shown in Fig. 6B. A positive bias of 3% was found when the commercial samples were analyzed; however, it was considered as acceptable for solids analysis. It could be concluded that the method developed was able to determine the polymorphic content of MFA in real samples.

3.2.2. MIR data analysis

As in the case of NIR, MIR spectra showed critical differences (Table 1) during the characterization of solid forms (Section 4.1). However, the presence of excipients may interfere with polymorphic quantitation. PLS emerging as a valid solution to resolve Form I and Form II in such complex matrix. MIR spectra were obtained

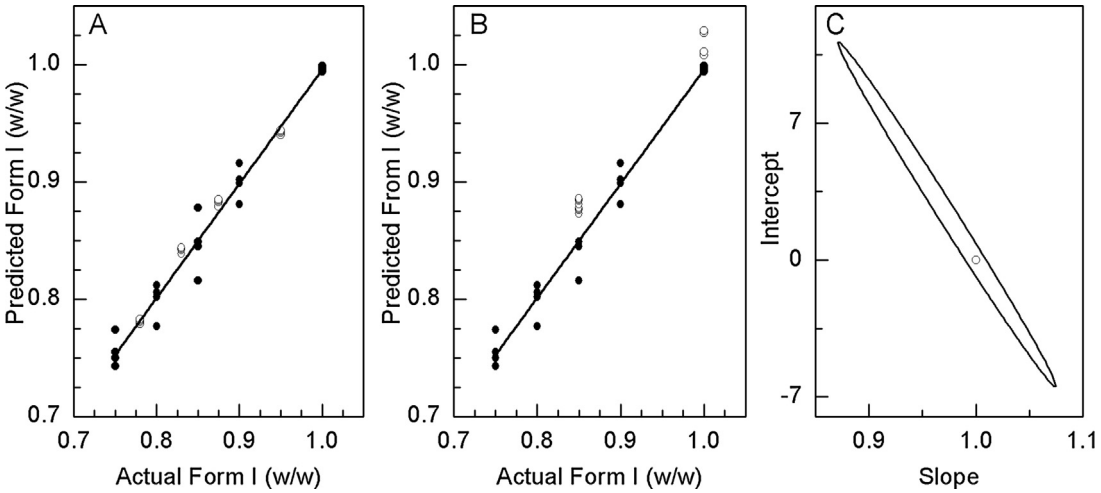

Fig. 6. Actual vs. predicted content of Form I (w/w), using the optimized NIR-PLS model. (A) Calibration (●) and validation (○) sets. (B) Commercial tablets with and without spiking (□) on calibration data (●). Ellipse of joint confidence region test for parameters of actual vs. predicted curve (C).

Table 3
Analytical summary of PLS models, calibration parameters and figures of merits. Validation set results.

Parameters	NIR	MIR
Calibration statistical summary		
Number of Samples	10	
Form I calibration levels (w/w)	0.750, 0.800, 0.850, 0.900, 1.00	
Spectral range (nm)	400–2500 nm	3500–750 cm^{-1}
PLS factors	5	5
Pretreatment	Centering	–
r^2	0.980	0.950
RMSD	1.42 10^{-4}	1.93 10^{-4}
Models' figures of merits		
Sensitivity	0.02	0.0029
Analytical sensitivity (γ; w/w^{-1})	2380	344
DMDC (γ^{-1}; w/w)	0.00042	0.0029
Selectivity	0.11	0.071
LOQ (w/w)	0.10	0.07
Results and statistic of validation set		
Number of samples	8	
Form I validation levels (w/w)	0.780, 0.830, 0.880, 0.9500	
Mean recovery (%)	100.4	104.3
Relative standard deviation (%)	1.0	8.2

RMSD, Root mean square deviation; DMDC, Detectable minimum difference of concentration; LOQ, Limit over quantification.

in 3500–400 cm^{-1} spectral range using the ATR accessory; however, 3500–750 cm^{-1} was selected as the working the range due to deleterious absorptions observed in 750–400 cm^{-1} range. Each sample was measured by in triplicate and the spectra obtained were averaged. The procedure was carried out twice for each sample. Calibration and validation samples were the same sets used in Section 3.2.1.

The optimal parameters were found following the minimum PRESS criterion during the cross-validation of Calibration set. Five PLS-factors and full spectra were found optimal paramethers.

The moving windows strategy [32] was also applied; although, no improvement of prediction was found by reduction of the spectral range. No spectral pretreatment was useful before PLS calculation. Table 3 summarizes PLS critical parameters and the figures of merits obtained during cross-validation.

The figures of merits (Table 3) were analyzed to verify the method suitability. An r^2 value of 0.950 and a RMSD value of 1.93% assure a good fitting of the method to the data. An actual vs predicted curve of Form I concentration was constructed for the validation set in order to evaluate accuracy and precision of the method (Fig. 7A). The curve constructed contained ideal curve (slope 1 and intercept 0) in their confidence region (Fig. 7B). Additionally, the average recovery of validation set (104.3%) was not statistically different to 100% [$T_{calculated} = 2.09$, $T_{(0.99;Df=15)} = 2.61$]; and SD (8.2%) was lower than 10%. The higher SD value might suggest a lower prediction ability of MIR spectroscopy in comparison to NIR.

When the commercial tablets were analyzed, Form I yielded 0.615 ± 0.06 w/w, showing both lower recovery (1.00 w/w expected) and higher dispersion than PLS-NIR methodology. In view of commercial sample recoveries, the spiked sample recoveries were not calculated.

Table 4
Parameters of the linear models for dissolution prediction.

Dissolution (%) at (min)	H_0[a]	β[b]	Prob.[c]	CV (%)[d]
5	–	–	NS	–
10	41.1	39	0.0348	6.0
15	48.7	45	0.0081	5.1
20	62.3	32	0.0099	3.6
25	73.3	21	0.0350	3.0
30	63.1	33	0.0002	2.1
45	73.9	23	0.0425	3.4
60	–	–	NS	–
90	–	–	NS	–

[a] Model coefficient.
[b] Intercept.
[c] *F* associated probability, P < 0.05 indicates significance of the model.
[d] Coefficient of variation (%). NS, not significant.

3.2.3. Data dissolution analysis – prediction of dissolution profiles

On the other hand, the information of dissolution was processed in order to predict the dissolution behavior of a pharmaceutical product, which may contain a mixture of polymorphs. This approach would work as a valid tool for product development into the paradigm of Quality by Design (QbD). Data were investigate to determine how polymorphic ratio (expressed as Form I content w/w) influenced dissolution rates, time by time. Table 4 shows the resulting models and the evaluation of its significance.

As expected, the model of the first dissolution time was not significant. This may be explained by the great variability inherent to the early stages of the dissolution, which hides the variation due to the polymorphs. As can be seen in Table 4, the dissolution rates for times between 10 and 45 min could be predicted by significant linear models. This is because the polymorphic content influences the dissolution beyond the inherent variation of the process.

The final stages of dissolution (60–90 min) cannot be modelled because they correspond to the plateau of dissolution. However,

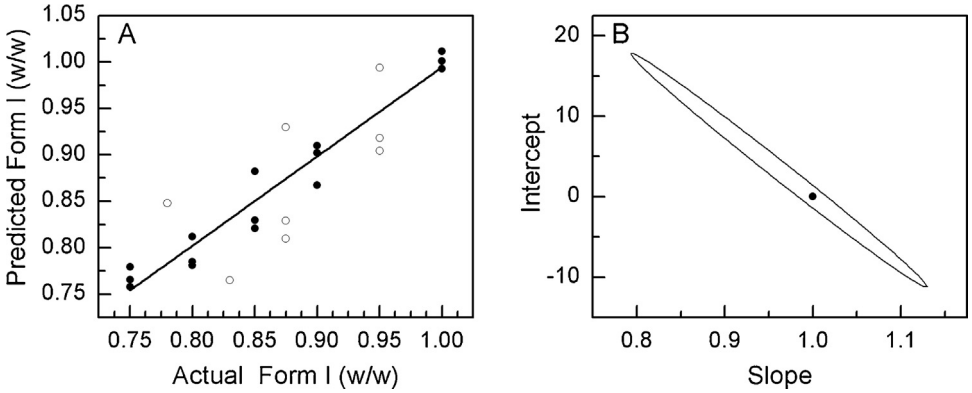

Fig. 7. Actual vs. predicted content of Form I (w/w), using the optimized MIR-PLS model for the calibration (●) and validation (○) sets (A). Ellipse of joint confidence region test for parameters of actual vs. predicted curve (B).

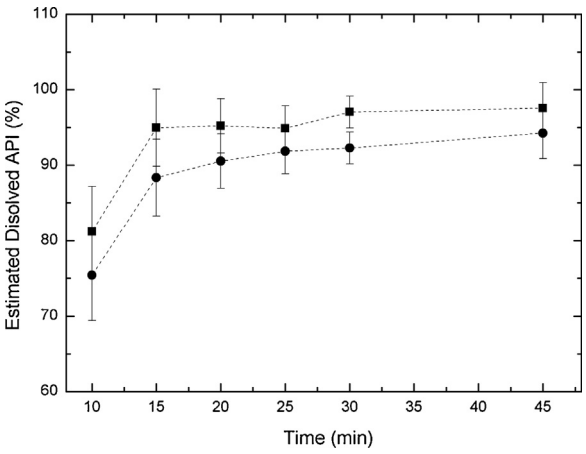

Fig. 8. Estimated dissolution profiles for commercial samples (■) and spiked commercial samples (●). Error bars shows the confidence range of estimation.

this dissolution rates could be represented by the mean of the measurements at these times.

The MLR models were used to estimate the dissolution profile of both commercial samples and spiked commercial samples, starting from Form I content calculated by NIR-PLS models (1.028 and 0.880 w/w, respectively). Fig. 8 shows estimated dissolution curves. Significant differences between two curves were observed since error bars did not contain the other estimated dissolution profile. Thus, a difference in polymorphic content of 10–15% may render dissolution profiles, which are not equivalent to each other.

The coupling of both methodologies, NIR-PLS/dissolution-estimation, implies the possibility to obtain dissolution profiles starting from simple NIR measurements when the polymorph ratio is the major variable.

4. Conclusions

This study aimed to develop easy and efficient methodologies to determine the polymorphic forms of MFA based on different analytical signals and chemometrics.

The complete characterization of two crystalline forms of MFA was carried out by thermal (DSC and melting point), spectroscopic (MIR and NIR) and physicochemical (dissolution performance and crystalline habits) monitoring. Critical differences were used to assign the identity of the obtained crystalline forms and commercial bulk drug (COM).

Taking into account the polymorph-differentiating properties of MIR and NIR spectroscopies, two PLS-based methods were developed. The critical parameters of the PLS of both models were optimized by cross-validation using minimum PRESS criteria. Calibrations showed no bias or systematic errors during prediction and the models yielded satisfactory recovery on validation sets ($100.4 \pm 1.0\%$ for NIR and $104.3 \pm 8.2\%$ for MIR), where MIR showed higher dispersion results. However, only NIR-PLS could satisfactorily predict Form I content in commercial samples and commercial spiked samples ($102.8 \pm 0.1\%$ and $103.5 \pm 0.5\%$, respectively).

The dissolution data of calibration samples were also analyzed in order to model the relationship among dissolution and polymorphic contents. The entire dissolution profile (average of 6 repetitions) of 10 calibration samples were used as MLR input. Significant correlations among polymorphic content and the dissolution of IFA in the range of 10–45 min were found. The significant models were used to predict dissolution profiles.

The conjunction of both models developed NIR-PLS and dissolution-estimation could act as a complementary tool in a QbD environment, to analyze the implication of polymorphic content in formulated products.

Acknowledgements

The authors gratefully acknowledge Consejo Nacional de Investigaciones Científicas y Tecnológicas (CONICET, Project PIP 2011-0471) and Secretaría de Ciencia y Tecnología de la UNR (SECyT-UNR, Projects BIO300 and BIO498) for financial support. We would like to thank the staff from the English Department (Facultad de Ciencias Bioquímicas y Farmacéuticas, Universidad Nacional de Rosario) for their assistance in the language correction of the manuscript.

References

[1] H.G. Brittain (Ed.), Polymorphism in Pharmaceutical Solids, 2nd ed., Informa Healthcare, Inc., NY, USA, 2009.
[2] L.S. Goodman, A. Gilman, The Pharmacological Basis of Therapeutics, 12th ed., Macmillan, New York, 2011.
[3] G. Ruoff, M. Lema, Strategies in pain management: new and potential indications for COX-2 specific inhibitors, J. Pain Symptom Manage. 25 (2003) 21–31.
[4] M. Van Eijkeren, H. Geuze, Effects of mefenamic acid on menstrual hemostasis in essential menorrhagia, Am. J. Obstet. Gynecol. 166 (1992) 1419–1428.
[5] A. Adam, L. Schrimpl, P.C. Schmidt, Some physicochemical properties of mefenamic acid, Drug Dev. Ind. Pharm. 26 (2000) 477–487.
[6] M. Otsuka, F. Kato, Y. Matsuda, Effect of temperature and kneading solution on polymorphic transformation of mefenamic acid during granulation, Solid State Ionics 172 (2004) 451–453.
[7] H.K. Chan, E. Doelker, Polymorphic transformation of some drugs under compression, Drug Dev. Ind. Pharm. 11 (1985) 315–332.
[8] S.S. Lekshmi, T.N. Guru Row, Conformational polymorphism in a non-steroidal anti-inflammatory drug, Mefenamic acid, Cryst. Growth Des. 12 (2012) 4283–4289.
[9] Y. Ashokraj, R. Panchagnula, T. Bapurao, P. Pillai, Mefenamic acid: new polymorph or crystal defect, Pharm Tech Eur. 18 (2006) 41–48.
[10] V.R.R. Cunha, C.M.S. Izumi, P.A.D. Petersen, A. Magalha˜es, M.L.A. Temperini, H.M. Petrilli, V.R.L. Constantino, Mefenamic acid anti-inflammatory drug: probing its polymorphs by vibrational (IR and raman) and solid-state NMR spectroscopies, J. Phys. Chem. B 118 (2014) 4333–4344.
[11] Council of Europe, European Pharmacopoeia, 6th ed., 2007, Strasbourg.
[12] V. Amaravathi, S. Firoz, D. Kishore, Formulation and evaluation of mefenamic acid tablets by using modified starch, Asian J. Pharm. Sci. Technol. 2 (2012) 46–53.
[13] V.P. Shah, G.L. Amidon, A theoretical basis for a biopharmaceutic drug classification: the correlation of in vitro drug product dissolution and in vivo bioavailability, Pharm. Res. 12 (1995) 413–420.
[14] C.E. Nicholson, S.J. Cooper, Crystallization of mefenamic acid from dimethylformamide microemulsions: obtaining thermodynamic control through 3D nanoconfinement, Crystals 1 (2011) 195–205.
[15] F. Kato, M. Otsuka, Y. Matsuda, Kinetic study of the transformation of mefenamic acid polymorphs in various solvents and under high humidity conditions, Int. J. Pharm. 321 (2006) 18–26.
[16] S. Romero, B. Escalera, P. Bustamante, Solubility behavior of polymorphs I and II of mefenamic acid in solvent mixtures, J. Pharm. 178 (1999) 193–202.
[17] A.J. Aguiar, J.E. Zelmer, Dissolution behavior of polymorphs of chloramphenicol palmitate and mefenamic acid, Int. J. Pharm. Sci. 58 (1969) 983–987.
[18] R. Panchagnula, P. Sundaramurthy, O. Pillai, S. Agrawal, Y. Ashok Raj, Solid-state characterization of mefenamic acid, J. Pharm Sci. 93 (2004) 1019–1029.
[19] G.P. Andrews, H. Zhai, S. Tipping, D.S. Jones, Characterization of the thermal, spectroscopic and drug dissolution properties of mefenamic acid and polyoxyethylene–polyoxypropylene solid dispersions, J. Pharm. Sci. 98 (2009) 4545–4556.
[20] C.V. Prasada Rao, M.V. Nagabhushanam, Enhancement of dissolution profile of mefenamic acid by solid dispersion technique, Int. Res. J. Pharm. Chem. 1 (4) (2011) 1127–1134.
[21] M.V. Nagabhushanam, A. Sudha Rani, Dissolution enhancement of mefenamic acid using solid dispersions in crospovidone, Int. J. Pharm. Pharm. Sci. 3 (2011) 16–19.
[22] M. Dixit, P.K. Kulkarni, Enhancing solubility and dissolution of mefenamic acid by freeze drying, Elixir Bio Phys. 39 (2011) 5026–5029.
[23] D.E. Bugay, Characterization of the solid-state: spectroscopic techniques, Adv. Drug Deliv. Rev. 48 (2001) 43–65.
[24] S. Cesur, S. Gokbel, Crystallization of mefenamic acid and polymorphs, Cryst. Res. Technol. 43 (2008) 720–728.
[25] R.K. Gilpin, W. Zhou, Infrared studies of the thermal conversion of mefenamic, acid between polymorphic states, Vib. Spectrosc. 37 (2005) 53–59.

[26] N.L. Calvo, R.M. Maggio, T.S. Kaufman, Chemometrics-assisted solid-state characterization of pharmaceutically relevant materials. Polymorphic substances, J. Pharm. Biomed. Anal. (2018) 518–537.
[27] M. Tsuka, J.I. Nishizawa, J. Shibata, M. Ito, Quantitative evaluation of mefenamic acid polymorphs by terahertz-chemometrics, J. Pham. Sci. 99 (2010) 4048–4053.
[28] United States Pharmacopeia Convention United States Pharmacopeia and National Formulary (USP 39–NF 34), 2015, Rockville.
[29] A. Burger, R. Ramberger, Thermodynamische Beziehungen zwischen polymorphen. Modifikationen: Flufenaminsiure und Mefenaminsiure, Mikrochim. Acta (1980) 17–28.
[30] T. Umeda, N. Ohnishi, T. Yokoyama, A kinetic study on the isothermal transition of polymorphic forms of tolbutamide and mefenamic acid in the solid state at high temperatures, Chem. Pharm. Bull. 33 (1985) 2073–2078.
[31] S. Jabeen, T. Dines, S. Leharne, B. Chowdhry, Raman and IR spectroscopic studies of fenamates. Conformational differences in polymorphs of flufenamic acid, mefenamic acid and tolfenamic acid spectrochim, Acta A Mol. Biomol. Spectrosc. 96 (2012) 972–985.
[32] L. Xu, I. Schechter, Wavelength selection for simultaneous spectroscopic analysis. Experimental and theoretical study, Anal. Chem. 68 (1996) 2392–2400.